Turbulence, Heat and Mass Transfer 4, 577-584
K. Hanjalić, Y. Nagano and M. Tummers (Editors)

Modifications of the $\overline{v^2} - f$ Model for Computing the Flow in a 3D Wall Jet

Lars Davidson[1], Peter V. Nielsen[2] and Andreas Sveningsson[1]

[1] *Dept. of Thermo and Fluid Dynamics, Chalmers University of Technology, SE-412 96 Göteborg, Sweden, http://www.tfd.chalmers.se/˜lada*

[2] *Dept. of Building Technology and Structural Engineering, Aalborg University, Sohngaards-holmsvej 57, DK-9000 Aalborg, Denmark*

Abstract —

In this work the flows in a three-dimensional wall jet and in a fully developed plane channel are computed. Two different turbulence models are used, the low-Re $k - \varepsilon$ model [1] and the $\overline{v^2} - f$ model [2, 3]. Two modifications of the $\overline{v^2} - f$ model are proposed. In the original model the wall-normal stress $\overline{v^2}$ is allowed to exceed $2k/3$, although it is supposed to be the smallest of the normal stresses. A simple modification of the $\overline{v^2} - f$ model is proposed which takes care of this problem.
In the $\overline{v^2} - f$ model, two velocity scales are available, $k^{1/2}$ and $(\overline{v^2})^{1/2}$, where the latter is the wall-normal fluctuations which are dampened by the wall. In the second modification of the $\overline{v^2} - f$ model we propose to use two viscosities, one ($\nu_{t,\perp}$) – based on $(\overline{v^2})^{1/2}$ – for the turbulent diffusion in the wall-normal direction, and the other ($\nu_{t,||}$) – based on $k^{1/2}$ – for the turbulent diffusion in the wall-parallel directions.

1. Introduction

In rooms ventilated with mixed ventilation the flow is usually supplied through an inlet device mounted on a wall just below the ceiling. The resulting flow is a wall jet developing along the ceiling. The flow in this wall jet determines the flow in the whole room. Thus it is very important to be able to predict the flow in the wall jet in order to be able to design the ventilation system.

The flow in an isothermal three-dimensional wall jet is the subject of the present work. It is well known that the spreading rates of a wall jet are very different in the wall-normal and the spanwise directions. The reason for this behavior is the presence of the wall which inhibits the turbulence in the wall-normal direction and hence also the spreading. According to the measurement [4], the spreading rates in the wall-normal and spanwise direction are $dy_{1/2}/dx = 0.065$ and $dz_{1/2}/dx = 0.32$, respectively. The large spreading rate in the spanwise direction is created by a strong secondary motion, generated by the normal stresses [5], analogous to how secondary motion in a square duct is generated. Whereas the magnitude of secondary motion in a square duct is approximately one percent of the streamwise velocity [6], the secondary motion in a three-dimensional wall jet is much larger. In [4] values of up to 18% (scaled with the local streamwise velocity) are reported, and predictions employing second-moment closures [5] show spanwise velocities of up to almost 30%.

In the present study we use a low-Re $k - \varepsilon$ model [1] and the $\overline{v^2} - f$ model [3]. Two modifications are proposed for the $\overline{v^2} - f$ model.

1. In the $\overline{v^2} - f$ model, a transport equation is solved for the wall-normal stress $\overline{v^2}$. The idea is to model the reduction of $\overline{v^2}$ as walls are approached. Thus $\overline{v^2}$ should be smaller than the other normal stresses, which means that $\overline{v^2} \leq 2k/3$. This relation is not satisfied in

Mesh	$\Delta x_{min},\ \Delta x_{max}$	$\Delta y_{min},\ \Delta y_{max}$	$\Delta z_{min},\ \Delta z_{max}$	$(N_y, N_z)_{in}$
1	$5.4 \cdot 10^{-4},\ 0.14$	$1.6 \cdot 10^{-4}, 0.045$	$4.3 \cdot 10^{-4},\ 0.015$	$21, 9$
2	$1.62 \cdot 10^{-3},\ 0.07$	$1.7 \cdot 10^{-4}, 0.039$	$2.1 \cdot 10^{-4},\ 0.027$	$31, 15$

Table 1: Details of the meshes. Number of grid points (N_x, N_y, N_z) for Mesh 1 & 2 are $(82, 92, 76)$ and $(112, 116, 82)$, respectively. Maximum stretching for Mesh 1 is $(f_x, f_y, f_z) = (1.1, 1.1, 1.07)$ and for Mesh 2 $(f_x, f_y, f_z) = (1.05, 1.08, 1.06)$. In the table are given minimum and maximum cell size in each direction and number of cells that cover the inlet, $(N_y \times N_z)_{in}$.

the standard $\overline{v^2} - f$ model. In the present work a simple modification is proposed which gives $\overline{v^2} \leq 2k/3$ everywhere. The modification is shown to work well in fully developed channel flow and for the 3D wall jet.

2. In the $\overline{v^2} - f$ model, two turbulent velocity scales are available, $(\overline{v^2})^{1/2}$ and $k^{1/2}$. In eddy-viscosity models – including the $\overline{v^2} - f$ model – the turbulent diffusion is modelled employing an isotropic turbulent viscosity using one turbulent velocity scale and one turbulent lengthscale. Since in the $\overline{v^2} - f$ model we have two turbulent velocity scales, the $\overline{v^2} - f$ model is in the present work modified so that one turbulent viscosity ($\nu_{t,\perp}$) – computed with $(\overline{v^2})^{1/2}$ – is used for the turbulent diffusion in the wall-normal direction, and another one ($\nu_{t,||}$) – computed with $k^{1/2}$ – is used for the turbulent diffusion in the wall-parallel directions.

The report is organized as follows. First a short description of the numerical method is presented. In the following section, the $\overline{v^2} - f$ model and the proposed modifications are described. Then the results are presented and discussed, and in the final section some conclusions are drawn.

2. Numerical Method

The finite volume computer program CALC-BFC (**B**oundary **F**itted **C**oordinates) for three-dimensional flow [7] is used in this study. The program uses collocated grid arrangement, Cartesian velocity components, and the pressure-velocity coupling is handled with SIMPLEC.

The convective terms in the momentum equations are discretized using the second-order, bounded van Leer scheme [8]. The convective terms in the equations for turbulent quantities are discretized with hybrid upwind/central differencing.

3. The $\overline{v^2} - f$ model

In [2] a modification of the $\overline{v^2} - f$ model was proposed allowing the simple explicit boundary condition $f = 0$ at walls. This model is used as standard model in the present work. The $\overline{v^2}$ and f-equations read [2]

$$\frac{\partial \bar{U}_j \overline{v^2}}{\partial x_j} = \frac{\partial}{\partial x_j}\left[(\nu + \nu_t)\frac{\partial \overline{v^2}}{\partial x_j}\right] + kf - 6\frac{\overline{v^2}}{k}\varepsilon \quad (1)$$

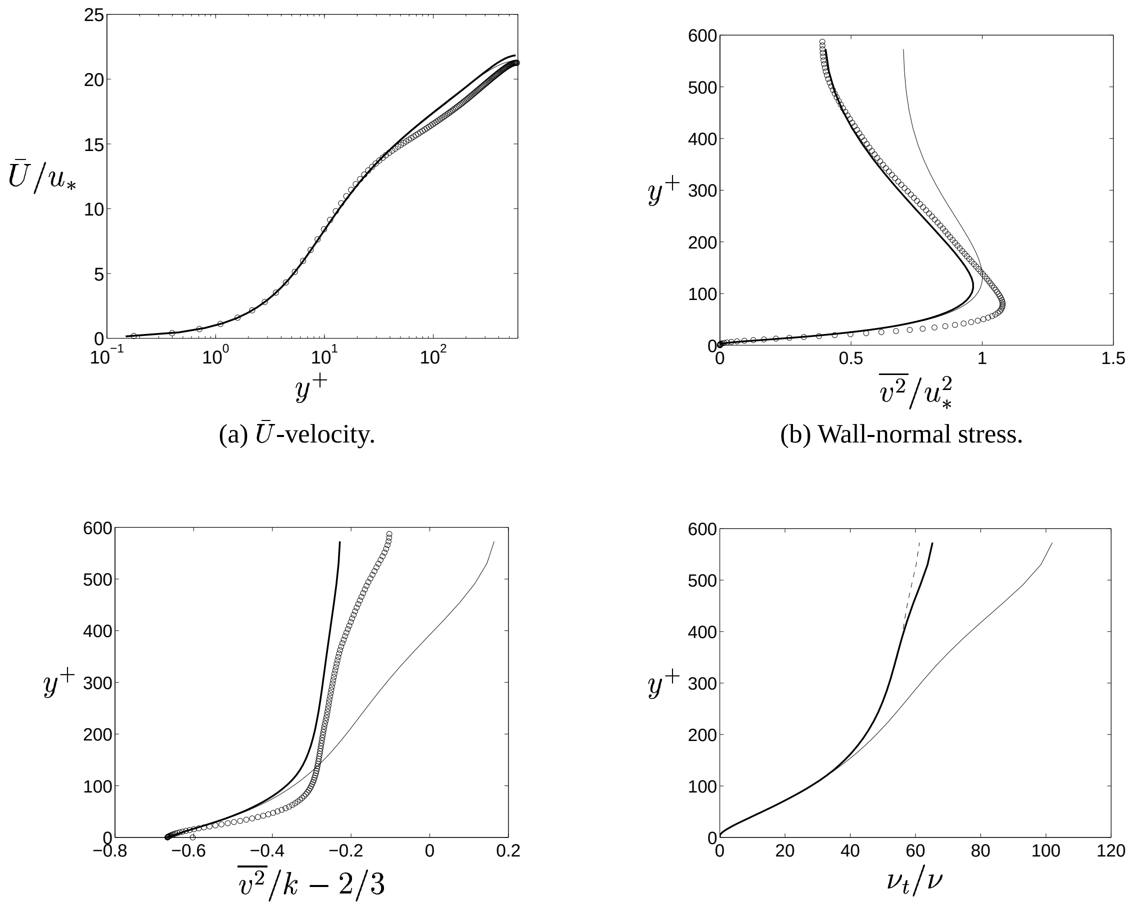

(a) $\bar{U}$-velocity.

(b) Wall-normal stress.

(c) Wall-normal anisotropy.

(d) Thick solid line line: Modification I, ν_t from Eq. 3; dashed line: Modification I and ν_t from Eq. 7.

Figure 1: Channel flow. $Re_\tau = 590$. $\overline{v^2} - f$ model. Thin solid line: standard model; thick solid lines: Modification I. Circles represent DNS [9]

$$
\begin{aligned}
&L^2 \frac{\partial^2 f}{\partial x_j \partial x_j} - f - \underbrace{\frac{1}{T}\left[(C_1 - 6)\frac{\overline{v^2}}{k} - \frac{2}{3}(C_1 - 1)\right]}_{\text{Term 1}} + \underbrace{C_2 \frac{P_k}{k}}_{\text{Term 2}} = 0 \\
&P_k = \nu_t \left(\frac{\partial \bar{U}_i}{\partial x_j} + \frac{\partial \bar{U}_j}{\partial x_i}\right)\frac{\partial \bar{U}_i}{\partial x_j} \qquad (2)\\
&T = \max\left\{\frac{k}{\varepsilon}, 6\left(\frac{\nu}{\varepsilon}\right)^{1/2}\right\},\ L = C_L \max\left\{\frac{k^{3/2}}{\varepsilon}, C_\eta\left(\frac{\nu^3}{\varepsilon}\right)^{1/4}\right\}
\end{aligned}
$$

The turbulent viscosity is computed from

$$\nu_t = C_\mu \overline{v^2} T \qquad (3)$$

The standard k and ε-equations are also solved (without damping functions). Boundary conditions at the walls are

$$k = \overline{v^2} = f = 0,\ \varepsilon = 2\nu k/y^2 \qquad (4)$$

The coefficients are given the following values:

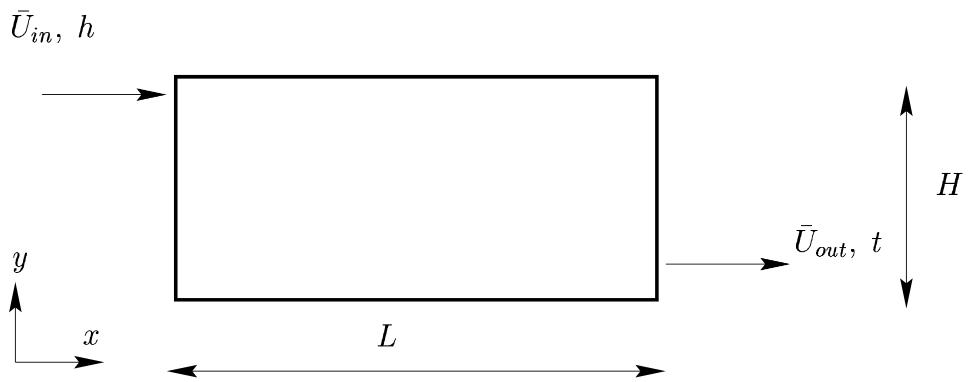

Figure 2: Configuration. $L = 3H$, $h/H = 0.01$, $t/H = 0.15$. $Re = \bar{U}_{in}h/\nu = 7000$.

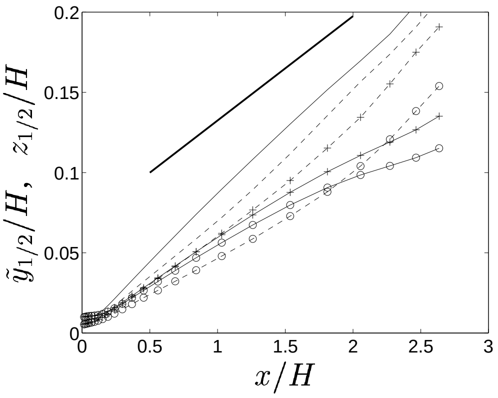

Figure 3: Spreading of the wall jet. Thick solid line: the slope $0.065x$. Thin solid line: $\tilde{y}_{1/2}$; dashed line: $z_{1/2}$; No markers: AKN model; $\circ$: $\overline{v^2} - f$ model, Modification I; $+$: $\overline{v^2} - f$ model, Modification I and II. Mesh 2.

C_μ	$C_{\varepsilon 2}$	σ_k	σ_ε	C_1	C_2	C_L	C_η
0.22	1.9	1	1.3	1.4	0.3	0.23	70

and $C_{\varepsilon 1} = 1.4(1 + 0.05(k/\overline{v^2})^{1/2})$.

Note that in the $\overline{v^2} - f$ model $\overline{v^2}$ denotes a generic wall-normal fluctuation component rather than the fluctuation in the y direction. This is achieved through the source ($= kf$) which is affected by the closest wall.

3.1. Modification I

The source term kf in the $\overline{v^2}$-equation (Eq. 1) is the modeled pressure strain term which is dampened near walls as f goes to zero. Since $\overline{v^2}$ represents the wall-normal normal stress, it should be the smallest normal stress, i.e. $\overline{v^2} \leq \overline{u^2}$ and $\overline{v^2} \leq \overline{w^2}$, and thus $\overline{v^2}$ should be smaller than $\frac{2}{3}k$. In the homogeneous region far away from the wall, the Laplace term is assumed to be negligible i.e. $\partial^2 f/\partial x_j \partial x_j \to 0$. Then Eq. 2 reduces to

$$f_{hom} = -\frac{1}{T}\left[(C_1 - 6)\frac{\overline{v^2}}{k} - \frac{2}{3}(C_1 - 1)\right] + C_2\frac{P_k}{k} \tag{5}$$

It turns out that in the region far away from the wall, the Laplace term is not negligible, and as a consequence $\overline{v^2}$ gets too large so that $\overline{v^2} > \frac{2}{3}k$. A simple modification is to set an upper bound on the source term kf in the $\overline{v^2}$-equation as

$$\overline{v^2}_{source} = \min\left\{kf, -\frac{1}{T}\left[(C_1-6)\overline{v^2} - \frac{2k}{3}(C_1-1)\right] + C_2 P_k\right\} \tag{6}$$

This modification ensures that $\overline{v^2} \leq 2k/3$. In regions where $\overline{v^2} \simeq 2k/3$, the turbulent viscosity with the $\overline{v^2}-f$ model is $2 \cdot 0.22k^2/(3\varepsilon) = 0.147k^2/\varepsilon$ (see Eq. 3) which is considerably larger than the standard value in the $k-\varepsilon$ model, $0.09k^2/\varepsilon$. A simple remedy is to compute ν_t as

$$\nu_t = \min\left\{0.09k^2/\varepsilon, 0.22\overline{v^2}T\right\} \tag{7}$$

Equations 6 and 7 are called "Modification I", unless otherwise stated.

3.2. Modification II

In the $\overline{v^2}-f$ model we have two velocity time scales, $(\overline{v^2})^{1/2}$ and $k^{1/2}$. The wall-normal stress $\overline{v^2}$ is dampened near walls as f goes to zero. Thus it is natural to introduce two viscosities, one for wall-normal diffusion ($\nu_{t,\perp}$) and one for diffusion parallel to the wall ($\nu_{t,||}$) In the present study, we propose to compute them as

$$\nu_{t,\perp} = 0.22\overline{v^2}T, \quad \nu_{t,||} = 0.09kT \tag{8}$$

For a wall parallel to the $x-z$ plane (for example), the turbulent diffusion terms are computed as

$$\frac{\partial}{\partial y}\left(\nu_{t,\perp}\frac{\partial\Phi}{\partial y}\right), \; \frac{\partial}{\partial x_j}\left(\nu_{t,||}\frac{\partial\Phi}{\partial x_j}\right), j \neq 2 \tag{9}$$

where Φ denotes a velocity component. Equation 9 could also be used for the turbulent quantities, but the effect is largest in the momentum equations, and in the present work Eq. 9 is used only in the momentum equations.

4. Results

4.1. Channel Flow

In Fig. 1 channel flow predictions are presented. The computations are carried out as 1D simulations, and the Reynolds number based on the friction velocity is $Re_\tau = u_*\delta/\nu = 590$, where δ denotes half-width of the channel. The number of cells used to cover half of the channel is 64, and a geometric stretching factor of 1.08 is used. The node adjacent to the wall is located at $y^+ = 0.14$.

From 1a it can be seen that the velocity profile is only very little affected by Modification I. The $\overline{v^2}$ profile is much better predicted with Modification I, as can be seen from Fig. 1b. Without the modification, $\overline{v^2}$ becomes too large for $y^+ > 150$, and it is also seen from Fig. 1c that $\overline{v^2}$ for $y^+ > 400$ erroneously becomes larger than $2k/3$.

Modification I reduces f [10]. The reason is that we have a positive feedback: the modification reduces $\overline{v^2}$ by reducing its source (Eq. 6), which in turn reduces f by reducing part of its source $(6-C_1)\overline{v^2}/k$, which further reduces the source in the $\overline{v^2}$ equation and so on.

The turbulent viscosity is presented in Fig. 1d using either Eq. 3 or Eq. 7. It can be seen that switching from the $\overline{v^2}-f$ expression (Eq. 3) to the $k-\varepsilon$ expression has only a small effect on the computed ν_t. For $y^+ > 380$ the viscosity from the $k-\varepsilon$ expression becomes larger than ν_t from the $\overline{v^2}-f$ model. The effect this switching has on the results in Fig. 1a-d are negligible.

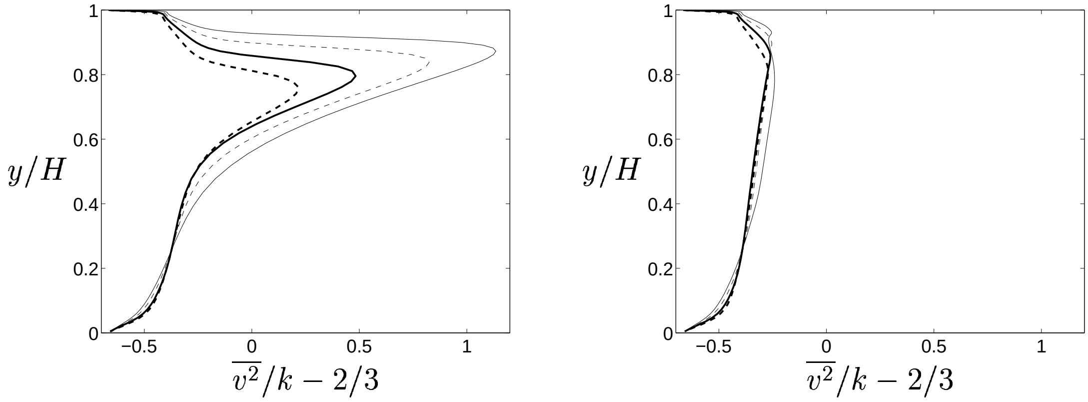

(a) Standard $\overline{v^2}-f$ model.

(b) $\overline{v^2}-f$ model, Modification I.

Figure 4: Profiles of $(\overline{v^2}/k-2/3)$ between $x/H=0.34$ and $x/H=1.07$. Thin solid line: $x/H=0.34$; thick dashed line: $x/H=1.07$. Comparison between standard $\overline{v^2}-f$ model and Modification I. Mesh 1.

4.2. The Wall Jet

The configuration is shown in Fig. 2. The square inlet is located at the uppermost part of the left wall and the outlet (a slot) is situated at the lowermost part of the right wall. Since the geometry is symmetric only half of the configuration is considered.

Two different grids have been used to check the grid independence of the computations, see Table 1. In [10] it was shown that the predictions are grid independent. In Fig. 3 the predicted half widths (defined as the position where $\bar{U}(x,y,z)$ is half of $\bar{U}_{max}(x)$) are presented. The spreading rates $d\tilde{y}_{1/2}/dx$ and $dz_{1/2}/dx$ for the AKN model are both larger than 0.065. This is in disagreement with experiment from where it is known that the spreading rate in the wall-normal direction (y) is much smaller than the one in the spanwise direction (z). The reason is that the turbulence in the wall-normal direction is dampened by the wall. The experimental values are $d\tilde{y}_{1/2}/dx=0.065$ and $dz_{1/2}/dx=0.32$ according to the measurement [4]. The predicted spreading rates for the $\overline{v^2}-f$ model, Modification I are also included in Fig. 3. It can be seen that, as expected, the predicted spreading of the wall jet is smaller with this $\overline{v^2}-f$ model than with the AKN model. The reason is that the wall-normal stress $\overline{v^2}$ in the $\overline{v^2}-f$ model is dampened by the reduced f as the wall is approached. When $\overline{v^2}$ is reduced, so is also the turbulent viscosity and thereby also the entrainment.

In Fig. 4 the effect of Modification I is investigated. It can be seen that without Modification I the predicted $\overline{v^2}$ becomes much larger than $2k/3$, which is physically incorrect. However, with Modification I, $\overline{v^2}\leq 2k/3$ as required. The effect on f is hardly noticeable, see [10]. As $\overline{v^2}$ is over-predicted, this also gives an over-predicted turbulent viscosity compared with a $k-\varepsilon$ model. ν_t is over-predicted with up to a factor of four in the outer shear layer of the wall jet compared with a $k-\varepsilon$ model, see [10]. Recall that in Modification I ν_t is computed from Eq. 7.

In [5] it was shown that the reason why the spreading rate in the lateral (z) direction is much larger than that in the wall-normal direction (y) is due to a strong secondary motion in the $y-z$ plane, driven by the anisotropy in the normal stresses. Thus a Reynolds stress model is required to predict this flow in a proper way [11]. One way to create anisotropic normal stresses in an eddy-viscosity model is to use anisotropic turbulent viscosities.

Below results using the $\overline{v^2}-f$ model with anisotropic turbulent viscosities are presented. In

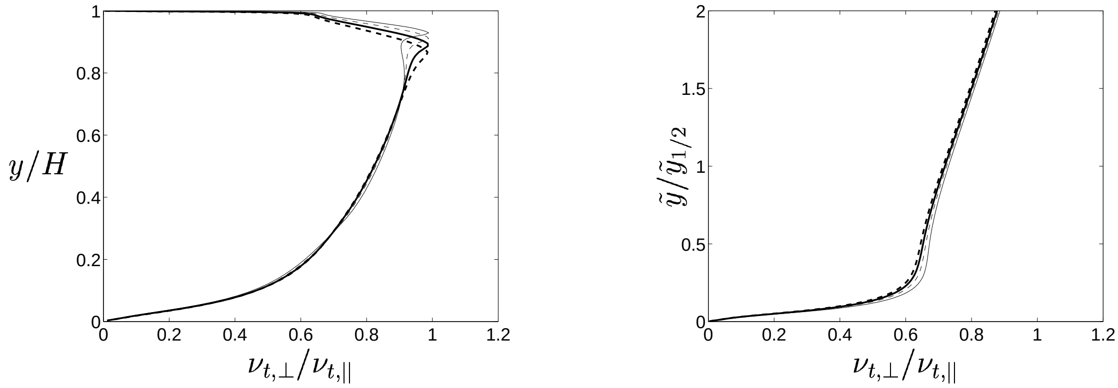

(a) Profiles between $x/H = 0.34$ and $x/H = 1.07$.

(b) Profiles between $x/H = 0.34$ and $x/H = 1.07$. $\tilde{y} = H - y$.

Figure 5: $\overline{v^2} - f$ model, Modification I and II. Mesh 2. $\nu_{t,\perp}/\nu_{t,||}$

Fig. 5 the predicted viscosity profiles are depicted for Modification I and II. In Modification II different viscosities are used for the diffusion terms in the wall-normal direction ($\nu_{t,\perp}$) and in the wall-parallel direction ($\nu_{t,||}$). The viscosity in the wall-normal direction is taken from the $\overline{v^2} - f$ model and the viscosity in the wall-parallel direction is computed with the $k - \varepsilon$ expression. The ratio between these viscosities is $\nu_{t,\perp}/\nu_{t,||} = 0.22\overline{v^2}/(0.09k)$, see Eq. 8. The expected effect is that the spreading of the wall jet in the spanwise direction with this modification should be larger than with Modification I. From Fig. 3 we find that this is indeed the case. Actually the spreading in the wall-normal direction has also increased somewhat, but clearly $z_{1/2}/\tilde{y}_{1/2}$ is larger for Modification I and II than for Modification I.

Profiles of the ratio $\nu_{t,\perp}/\nu_{t,||}$ are shown in Fig. 5. It can be seen that $\nu_{t,\perp}$ is much smaller than $\nu_{t,||}$. The ratio $\nu_{t,\perp}/\nu_{t,||}$ is approximately 0.6 at the location of the velocity peak ($\tilde{y}/\tilde{y}_{1/2} \simeq 0.15$). Inside the velocity peak the ratio goes to zero as $\overline{v^2}$ is dampened by wall ($f \to 0$).

5. Conclusions

Two modifications of the $\overline{v^2} - f$ model have been presented. In the first modification – Modification I – the source term in the $\overline{v^2}$ equation is limited so as to ensure that $\overline{v^2} < 2k/3$. The second modification – Modification II – is based on a non-isotropic eddy-viscosity approach. Different viscosities are used for the turbulent diffusion in the wall-normal direction and in the wall-parallel directions. The object of Modification II was to be able to model the different spreading rates in the wall-normal and spanwise direction of a 3D wall jet.

Modification I was shown to work well. The predicted $\overline{v^2}$ was smaller than $2k/3$ both for the fully developed channel flow and the 3D wall jet. Modification II was found to give only a small improvement for the 3D wall jet, and with this modification the spanwise spreading rate was increased.

A further modification of the $\overline{v^2} - f$ could be to use the limitation of the time scale T model derived from the requirement that the normal stresses must stay positive in regions of large irrotational strains (e.g. in stagnation regions) [12]. It is very important that this limitation is imposed in a consistent manner in Eqs. 1 and 2. Furthermore, the limitation has a strong effect also in region far away from stagnation regions. For more details, see Refs. [13, 14].

References

1. K. Abe, T. Kondoh, and Y. Nagano. A new turbulence model for predicting fluid flow and heat transfer in separating and reattaching flows - 1. Flow field calculations. *Int. J. Heat Mass Transfer*, 37:139–151, 1994.
2. F-S Lien and G. Kalitzin. Computations of transonic flow with the v2f turbulence model. *International Journal of Heat and Fluid Flow*, 22(1):53–61, 2001.
3. P.A. Durbin. Near-wall turbulence closure modeling without damping functions. *Theoretical and Computational Fluid Dynamics*, 3:1–13, 1991.
4. H. Abrahamsson, B. Johansson, and L. Löfdahl. The turbulence field of a fully developed three-dimensional wall jet. Report 97/1, Dept. of Thermo and Fluid Dynamics, Chalmers University of Technology, Gothenburg, 1997.
5. T.J. Craft and B.E. Launder. On the spreading mechanism of the three-dimensional turbulent wall jet. *Journal of Fluid Mechanics*, 435:305–326, 2001.
6. J. Pallares and L. Davidson. Large-eddy simulations of turbulent flows in stationary and rotating channels and in a stationary square duct. Report 00/03, Dept. of Thermo and Fluid Dynamics, Chalmers University of Technology, 2000.
7. L. Davidson and B. Farhanieh. CALC-BFC: A finite-volume code employing collocated variable arrangement and cartesian velocity components for computation of fluid flow and heat transfer in complex three-dimensional geometries. Rept. 95/11, Dept. of Thermo and Fluid Dynamics, Chalmers University of Technology, Gothenburg, 1995.
8. B. van Leer. Towards the ultimate conservative difference scheme. Monotonicity and conservation combined in a second order scheme. *Journal of Computational Physics*, 14:361–370, 1974.
9. R.D. Moser, J.D. Kim, and N.N. Mansour. Direct numerical simulation of turbulent channel flow up to $Re_\tau = 590$. *Physics of Fluids A*, 11:943–945, 1999.
10. L. Davidson and P.V. Nielsen. Comparing a $k - \varepsilon$ model and the $v^2 - f$ model in a 3D isothermal wall jet. Report R0301, Dept. of Building Technology and Structural Engineering, Aalborg University, Aalborg, Denmark, 2003.
11. A. Schälin and P.V. Nielsen. Impact of turbulence anisotropy near walls in room air flow (accepted for publication). *International Journal of Indoor Environment and Health*, 2003.
12. P.A. Durbin. On the $k - 3$ stagnation point anomaly. *International Journal of Heat and Fluid Flow*, 17:89–90, 1996.
13. A. Sveningsson. Analysis of the performance of different $\overline{v^2} - f$ turbulence models in a stator vane passage flow. Thesis for licentiate of engineering, Dept. of Thermo and Fluid Dynamics, Chalmers University of Technology, Göteborg, Sweden, 2003.
14. A. Sveningsson and Lars Davidson. Assessment of realizability constraints and boundary conditions in $\overline{v^2} - f$ turbulence models (to be presented). In *4th Int. Symp. on Turbulence Heat and Mass Transfer*, Antalya, Turkey, 2003.